Environmental Science & Technology

pubs.acs.org/est

Article

Provenance of Anthropogenic Pb and Atmospheric Dust to Northwestern North America

Bess G. Koffman,* Patrick Saylor, Roujia Zhong, Lily Sethares, Meg F. Yoder, Lena Hanschka, Taylor Methven, Yue Cai,* Louise Bolge, Jack Longman, Steven L. Goldstein, and Erich C. Osterberg

Cite This: *Environ. Sci. Technol.* 2022, 56, 13107−13118

Read Online

ACCESS | Metrics & More | Article Recommendations | Supporting Information

ABSTRACT: Industrial activities release aerosols containing toxic metals into the atmosphere, where they are transported far from their sources, impacting ecosystems and human health. Concomitantly, long-range-transported mineral dust aerosols play a role in Earth's radiative balance and supply micronutrients to iron-limited ecosystems. To evaluate the sources of dust and pollutant aerosols to Alaska following the 2001 phase-out of leaded gasoline in China, we measured Pb-Sr-Nd isotopic compositions of particles collected in 2016 from snow pits across an elevational transect (2180−5240 m-a.s.l) in Denali National Park, USA. We also determined Pb flux and enrichment from 1991−2011 in the Denali ice core (3870 m-a.s.l). Chinese coal-burning and non-ferrous metal smelting account for up to 64% of Pb deposition at our sites, a value consistent across the western Arctic. Pb isotope ratios in the aerosols did not change between 2001 and 2016, despite the ban on lead additives. Emissions estimates demonstrate that industrial activities have more than compensated for the phase-out of leaded gasoline, with China emitting ~37,000 metric tons year^{-1} of Pb during 2013−2015, approximately 78% of the Pb from East Asia. The Pb flux to Alaska now equals that measured in southern Greenland during peak pollution from North America.

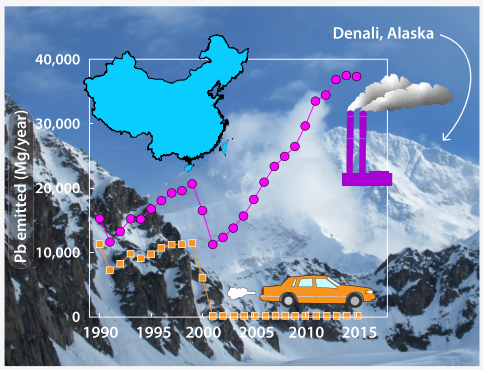

KEYWORDS: *Sr-Nd-Pb isotopes, air pollution, ice core, lead emissions, lead flux, Alaska, China, North Pacific*

INTRODUCTION

Atmospheric aerosols derived from anthropogenic and natural sources have wide-ranging effects on ecosystems, humans, and Earth's climate. One of the most pervasive environmental pollutants, lead (Pb), is a toxic heavy metal that has detrimental impacts on both human health and ecosystems.[1,2] The majority of modern atmospheric Pb is emitted through human activities,[3,4] including combustion of leaded gasoline (phased out globally as of 2021[5]), coal-burning, industrial activities, waste incineration, and non-ferrous metal mining and smelting.[6,7] In addition to these anthropogenic sources, natural volcanic and dust emissions deliver small quantities of Pb to the environment. Fresh snow on a glacier surface acts as a natural aerosol sampler, trapping particles through both wet (e.g., scavenging, cloud condensation nuclei) and dry deposition. Importantly, there are no significant sources of aerosols to a pristine snow surface besides the atmosphere. Thus, measurements from glacier surfaces can augment direct atmospheric measurements by providing temporally resolved archives of atmospheric particle deposition from remote locations. Ice cores from Greenland and the European Alps document significant declines in Pb deposition following the bans on leaded gasoline in Europe and North America;[8−10] however, new records of atmospheric deposition are needed in order to track the history of Pb emissions in other regions of the world. Existing snow and ice Pb isotope data from northwestern North America only extend to 2001 (refs 11 and 12), and thus changes in Pb pollution sources to this region following the 2001 phase-out of leaded gasoline in China have not been documented.

In addition to the atmospheric transport of heavy metals, mineral dust from desert and glacial sources has far-reaching impacts and can be observed far downwind from its source regions. Mineral dust in the atmosphere affects Earth's radiative balance by scattering short-wave and absorbing long-wave radiation; net effects on surface temperature are largely dependent on grain size and are now thought to be positive, causing ~0.15 W m^{-2} warming,[13,14] equivalent to about 9% of the radiative forcing from anthropogenic CO_2 in 2011. Dust also delivers iron and other micronutrients to offshore regions of the ocean, where primary production is often iron-limited.[15,16] Dust and pollution aerosols both serve as cloud condensation nuclei, affecting cloud distribution and

Received: May 25, 2022
Revised: August 29, 2022
Accepted: August 29, 2022
Published: September 9, 2022

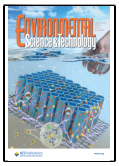

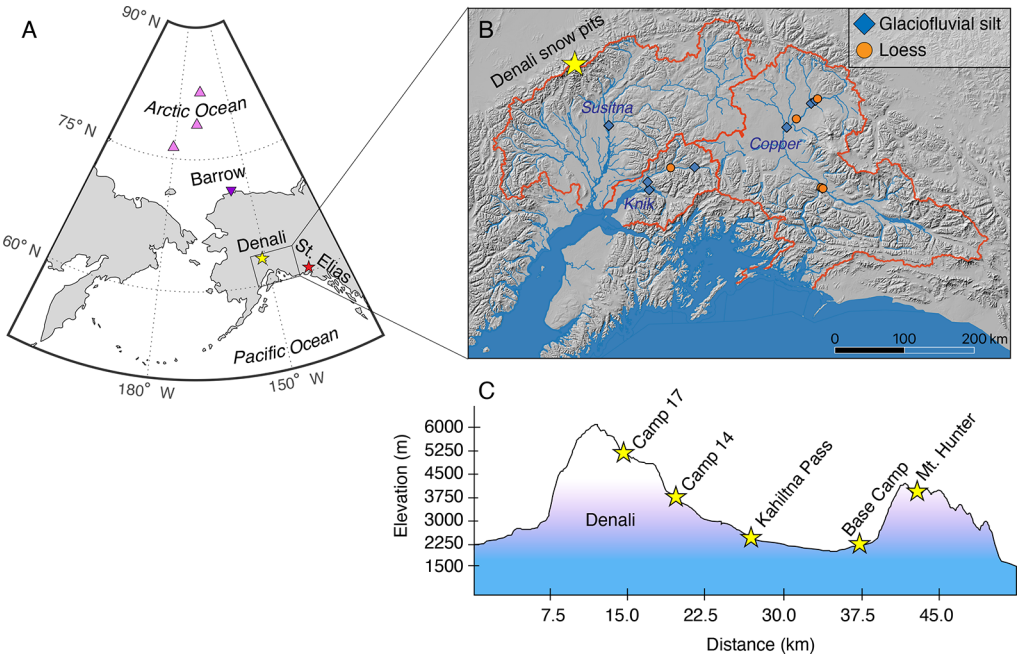

Figure 1. Maps showing sites discussed in the text. (A) Overview map showing snow pit sampling locations: Denali (yellow star, this study), the St. Elias mountains (red star[11,12,23]), and Barrow, Alaska and the Chukchi Sea sector of the Arctic Ocean (triangles[22]). (B) Digital elevation model showing locations of sediments collected to characterize local dust source compositions. Samples were collected from the three major drainages of southcentral Alaska: the Susitna, Knik, and Copper Rivers. (C) Schematic topographic profile showing snow pit elevations in Denali National Park. Mt. Hunter is also the site of the Denali deep ice core used to estimate Pb flux and enrichment.

precipitation patterns.[17−19] Provenance studies provide critical constraints on the sources, transport pathways, and magnitudes of deposition of dust and heavy metals, helping to constrain potential impacts of dust and anthropogenic pollutant aerosols on humans, ecosystems, and the climate.

To assess the sources of pollution alongside both local and long-range-transported mineral dust aerosols, we collected surface snow from an elevation transect in Denali National Park, Alaska, USA, in June 2016 (Figure 1). We combine strontium (Sr), neodymium (Nd), and Pb isotopic measurements to fingerprint dust and pollution aerosols and trace them to their source regions. We also characterize the compositions of dust produced by glacier erosion in southcentral Alaska and Yukon Territory, Canada, using 20 glaciofluvial silt and loess samples (Figure 1). Our approach allows for five-dimensional geochemical discrimination of dust and pollution sources to the central Alaska Range (i.e., Sr, Nd, and up to 3 different Pb isotope ratios), assessing both spatial and elevational gradients in dust and pollution aerosol deposition in spring 2016. We also present Pb concentration, enrichment, and flux data spanning 1991−2011 from the Denali ice core drilled in 2013 (refs 20, and 21). The results represent the first assessment of Pb pollution sources to northwestern North America since the phase-out of leaded gasoline in China in 2001. Comparison with published records from Barrow, Alaska and the Arctic Ocean,[22] the St. Elias Mountains of Yukon, Canada,[11,12,23] the Devon Ice Cap in Nunavut, Canada,[24] and from Greenland[25−28] allows for a broader assessment of dust and pollution sources to the western Arctic.

MATERIALS AND METHODS

Isotopic 'Fingerprinting' Approach. Analysis of Sr, Nd, and Pb isotope compositions of particles preserved in snow and glacier ice allow tracing to their source through isotopic 'fingerprinting'. This well-established approach benefits from the following attributes: (1) differing rock compositions and geologic histories result in distinctive bedrock Sr-Nd-Pb isotope compositions; (2) sediment and aerosol Sr-Nd-Pb compositions reflect those of their terrestrial and anthropogenic sources; and (3) these isotope ratios do not chemically fractionate during transport or geochemical processing. However, heterogeneity among the mineral distributions may result in some isotopic heterogeneity among different grain size fractions, which in particular has been observed to impact Sr and Pb isotopes.[29−31] To mitigate the effects of physical sorting on Sr and Pb isotope ratios, we follow the common approach of using the <5 μm size fraction to characterize the southcentral Alaska dust source region.[32]

Snow Pits and Sediments. In 2016 and 2017, we collected 20 fine-grained sediment samples from the major drainages of southcentral Alaska (Figure 1B), as well as from the vicinity of Kluane Lake, Yukon Territory, Canada. Samples include glaciofluvial silt and locally derived loess, which together represent glaciogenic sediments from these catchments. Locations and a full suite of major and trace element data, as well as detailed iron geochemistry, have been published previously, and data are available through the EarthChem Library:[33,34] https://ecl.earthchem.org/view.php?id=1679. Snow pit samples were collected from an elevational transect of sites (2180 to 5240 m a.s.l.) in Denali National Park, Alaska (Figure 1). We sampled in June 2016, and the samples represent springtime deposition, the season when Asian dust emissions are at their highest.[35] More information on sampling protocols, assessment of seasonality, grain size distributions, and determination of the potential contribution of volcanic ash from the March 2016 Pavlof eruption can be found in the SI.

https://doi.org/10.1021/acs.est.2c03767
Environ. Sci. Technol. 2022, 56, 13107−13118

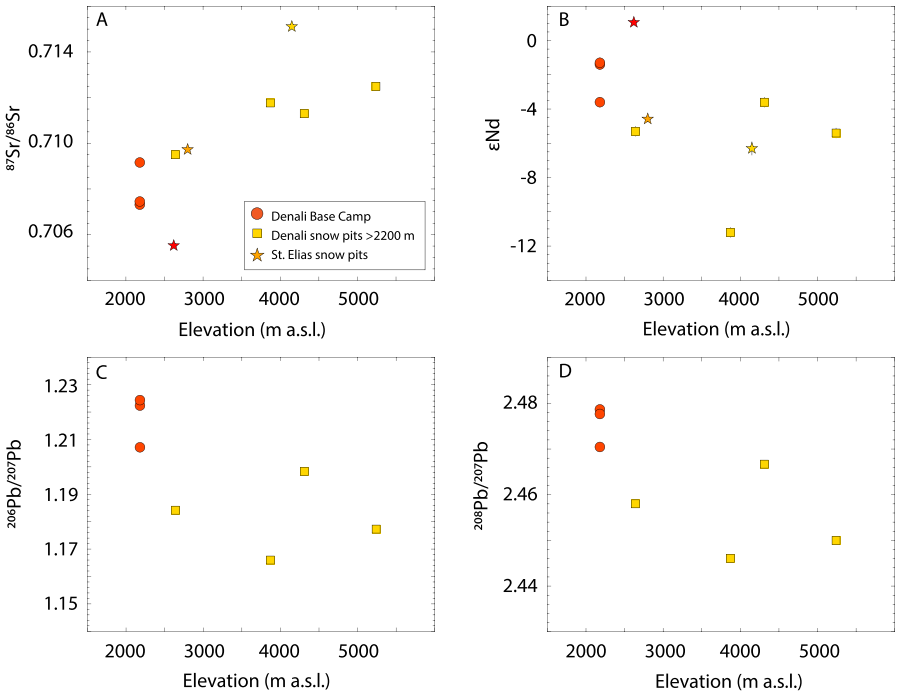

Figure 2. Snow pit Sr-Nd-Pb isotope data from Denali and the St. Elias[12] plotted as a function of elevation. (A) $^{87}Sr/^{86}Sr$, (B) εNd, (C) $^{206}Pb/^{207}Pb$, and (D) $^{208}Pb/^{207}Pb$. The elevation dependence reflects aerosol contributions from different mixing ratios of sources at different elevations. Error bars are plotted where they are greater than symbol size.

Following laboratory processing (see the SI), filtered snow pit dust and <5 μm sediment samples were digested on a hotplate under HEPA filtration using HF + HNO_3, with $HClO_4$ added if needed to oxidize organic carbon. Sr, Nd, and Pb aliquots were separated using chromatographic columns (see the SI), and isotope ratios were measured on a Neptune Plus multicollector inductively coupled plasma mass spectrometer (MC-ICP-MS) at the Lamont-Doherty Earth Observatory. Full analytical details, including blanks, standard values, and reproducibility can be found in the SI. Sediment and snow pit Sr-Nd-Pb isotope data can be accessed through the EarthChem Library at https://ecl.earthchem.org/view.php?id=2229.

Denali Ice Core. We use data from an ice core drilled in Denali National Park to estimate the Pb flux and enrichment over the period 1991−2011, excluding explosive eruptions (see the SI for details). A parallel pair of cores were drilled 208 m to bedrock on the Mt. Hunter summit saddle (Figure 1) in 2013 (refs 20 and 21). The timescale for this interval was developed using annual layer counting and has an age uncertainty of <0.5 yr.[20] In this study, we use Denali core 2. The ice core was melted using a continuous melting system[36,37] at Dartmouth College, with discrete samples collected for ICP-MS and other analyses. These were acidified to 1% v/v with Optima-grade nitric acid and allowed to leach at room temperature for at least 6 weeks before analysis to achieve stable concentrations with the nitric acid leach.[38] Lead concentrations were analyzed using ^{208}Pb in low-resolution mode on a Thermo-Finnigan Element II high-resolution ICP-MS at the University of Maine.

Lead Emissions Estimates. Following the approach of ref 39, we developed Pb emissions estimates for China, Japan, South Korea, and Russia using non-ferrous metal (Cu, Ni, Pb, Zn) smelting data from the USGS Mineral Yearbook (https://www.usgs.gov/centers/national-minerals-information-center/commodity-statistics-and-information) and coal-burning data from the World Bank Open Data database (https://data.worldbank.org/); see the SI for details.

RESULTS AND DISCUSSION

Dust Provenance in Denali National Park and the Western Arctic. Northwestern North America, with significant glaciated landscapes in Alaska, British Columbia, and the Yukon Territory, is both a source of glaciogenic dust and a repository of local and long-range-transported dust and pollution. Satellite and surface aerosol observations have provided clear evidence of trans-Pacific dust transport from the deserts of China and Mongolia to the region.[35,40−42] Moreover, dust from the deserts of China has been documented around the Northern Hemisphere.[32,41,43,44] Local dust sources are also important as river valleys draining glaciated catchments in southcentral Alaska supply dust to the iron-limited waters of the Gulf of Alaska.[45,46]

Dust source regions and Pb pollution sources show significant variations in Sr-Nd-Pb isotopic compositions across the Northern Hemisphere.[32,47] Among global pollution and dust sources, Chinese Pb ore has a distinctly high thorogenic composition (i.e., high $^{208}Pb/^{204}Pb$ and $^{208}Pb/^{207}Pb$).[7,47] In addition, Chinese coal Pb can be distinguished isotopically from both European and North American coal sources.[48] Isotopic fingerprinting therefore provides a robust approach for discerning among key potential Pb pollution and dust sources in the Northern Hemisphere, providing information on atmospheric transport pathways independent of satellite observations and back-trajectory or transport modeling.

The combination of Sr-Nd-Pb isotopes allows for the separation of dust and pollution signals. We use Sr and Nd isotopes to characterize the dust component of aerosol deposition, as these isotopes are minimally influenced by pollution sources. The Denali snow pit samples display a range of Sr-Nd isotope compositions that varies with elevation

https://doi.org/10.1021/acs.est.2c03767
Environ. Sci. Technol. 2022, 56, 13107−13118

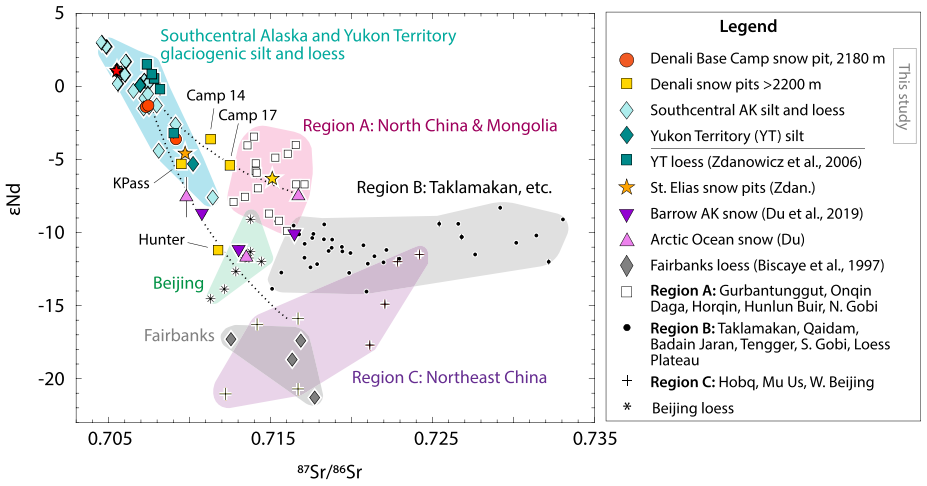

Figure 3. Snow pit Sr-Nd isotope compositions from Alaska, the St. Elias,[12] and the western Arctic[22] compared to potential dust source regions.[31,49,50] St. Elias snow pit elevations are as follows: red star, 2620 m; orange star, 2800 m; yellow star, 4150 m a.s.l. Barrow and Arctic Ocean samples are from sea level. The dotted lines show calculated mixtures of southcentral Alaska dust with Region A and Region C desert sediments that could plausibly produce several of the observed snow pit dust compositions. Beijing loess data are shown for context but are not considered an independent source region. Source region data include the <5 μm fraction from refs 31 and 50and the HOAc-residue fraction from ref 49. Error bars are generally smaller than symbols. Camp 14 data have been corrected to remove a volcanic contribution (see the SI).

(Figure 2). Samples from Denali Base Camp (2180 m) have lower $^{87}Sr/^{86}Sr$ (0.7073−0.7092) and higher εNd (−3.6 to −1.3), while samples from Camp 17 (5240 m) and Mt. Hunter (3870 m) have higher $^{87}Sr/^{86}Sr$ (0.7118−0.7125) and lower εNd (−11.2 to −5.4) (Figure 2). Other sites on the Denali massif (elevations 2640 and 4310 m) have intermediate Sr-Nd compositions. The Camp 14 sample (4310 m) appears to contain a contribution of ash from the March 2016 eruption of Pavlof Volcano in the Aleutian Islands (see the SI). Removing this contribution to the Sr-Nd composition shifts the data toward higher $^{87}Sr/^{86}Sr$ (0.7113) and lower εNd (−3.6), as would be expected for this relatively high-elevation site. The elevational trends are comparable to those observed in the St. Elias[12] (Figure 2).

Low-elevation snow pit samples are indistinguishable from local glaciogenic sediments (Figure 3), suggesting that dust transported from the glacier-fed river valleys of southcentral Alaska reaches elevations of at least 2100 m. (See the SI for a detailed characterization of local dust source areas). At higher elevations (2640−5240 m), we see an increasing contribution from an isotopically older crustal end-member, indicated by higher $^{87}Sr/^{86}Sr$ and lower εNd values (Figure 3). Given isotopic similarities, the predominance of Asian dust in the North Pacific atmosphere,[35,40] and previous geochemical analyses of dust deposited in northwestern North America,[12] we infer this end-member to be desert dust from China and Mongolia.

The dust reaching high-elevation sites in the Alaska and St. Elias ranges can be traced back to Asian desert source regions using Sr-Nd isotopes (Figure 3). The differing Sr-Nd isotopic compositions of these deserts reflect the region's tectonic history and derivation of sediments from cratons of different crustal residence age. One sample from Denali (Camp 17, 5240 m) and one from Mt. Logan (King Col, 4150 m, yellow star in Figure 3)[12] are compatible with a North China desert source, with $^{87}Sr/^{86}Sr > 0.713$ and εNd ≈ −6 (ref.[24]). This region, labeled 'Region A' in Figure 3, includes the Gobi, Gurbantunggut, Onqin Daga, Horqin, and Hunlun Buir deserts and sandy lands, which are derived from the North China Craton and associated sediments.[32,49,50] The Mt. Hunter, Alaska, sample (3870 m) has a more negative εNd value of −11, lower than the values from 'Region A' deserts. Its most likely Asian source is the deserts and sandy lands of northeastern China ('Region C' in Figure 3), which include the Hobq and Mu Us deserts and the region of western Beijing. This region is characterized by $^{87}Sr/^{86}Sr$ of 0.712−0.725 and lower εNd-values of −21 to −12, reflecting the erosion of older crustal materials associated with the Ordos craton.[49,50] The relatively low $^{87}Sr/^{86}Sr$ ratio of the Mt. Hunter sample (0.7118) argues against the Taklamakan and Southern Gobi region ('Region B' in Figure 3) as its main source region as dust from these regions is characterized by $^{87}Sr/^{86}Sr$ of 0.715−0.733 and εNd of −12 to −8 (refs 49 and 50), including the Qaidam Basin, Badain Jaran and Tengger deserts, and the Chinese Loess Plateau. While our spring 2016 samples appear to reflect the inputs of a subset of desert regions, we expect that on longer timescales, dust deposition in northwestern North America reflects inputs from many or all of these East Asian deserts.

Loess in the Fairbanks, Alaska region (northeast of Denali) also carries an older crustal isotopic signature, similar to the deserts of 'Region C' in northeastern China[32] (Figure 3). However, we think it is unlikely that this dust would be lofted up and over the Alaska Range, given prevailing wind patterns, so this source probably supplies only minor contributions to our sites, at most. On the whole, we conclude that the measured Sr-Nd compositions at higher elevations reflect significant contributions of dust from the deserts of northern and northeastern China.

Surprisingly, even at elevations of ∼4000 m, isotope mixing calculations reveal that sites in the Alaska Range receive dust from both southcentral Alaska river valleys and Asian desert sources. We use a 2-component concentration-dependent isotope mixing equation to estimate source contributions, following the general form:

https://doi.org/10.1021/acs.est.2c03767
Environ. Sci. Technol. 2022, 56, 13107−13118

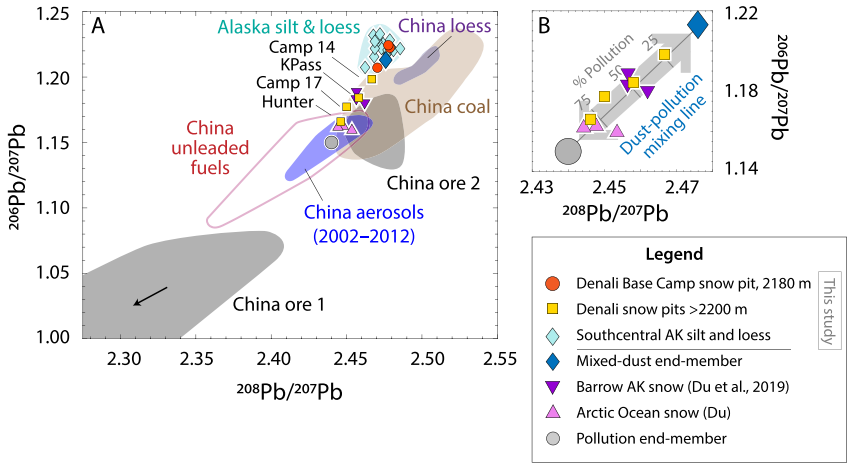

Figure 4. $^{206}Pb/^{207}Pb$ vs $^{208}Pb/^{207}Pb$ of Alaska and Arctic snow pit samples[22] compared to potential dust[31,51] and pollution[43,52,53,55] sources. Denali Base Camp samples fall within the field of southcentral Alaska glaciogenic sediments (A), while higher-elevation samples follow a mixing line between a mixed-dust end-member and a pollution end-member (B). Barrow, Alaska and Arctic Ocean snow samples follow a similar trend,[22] and Arctic samples are indistinguishable from Chinese aerosols. The mixed-dust end-member represents an ~60/40 mixture of southcentral Alaska and Asian dust source sediments, based on the Sr-Nd isotope data. The pollution end-member, with $^{206}Pb/^{207}Pb$ of 1.1542 and $^{208}Pb/^{207}Pb$ of 2.4386, is calculated using ice core Pb enrichment data from Mt. Hunter, assuming the other Pb source is the mixed-dust end-member (see text). China unleaded fuels are shown for reference but are not considered a major Pb source. Error bars on samples from this study represent 2σ external errors and are smaller than the symbol size.

$$Mix_{AB} = [R_A \times C_A \times f_A + R_B \times C_B \times f_B] / [C_A \times f_A + C_B \times f_B]$$

where Mix_{AB} is the isotope ratio of a given mixture of end-members A and B; R is the isotope ratio of an end-member; C is the concentration of the element of interest in that end-member; and f represents the fraction of the mixture contributed by each end-member. Depending on the sample, we estimate that Asian deserts supply anywhere from ~35 to 75% of the dust to our sites (Table S2). This implies a significant role for locally sourced dust. Our results thus suggest that deep ice cores drilled at high-elevation sites in the Alaska and St. Elias ranges can be used to reconstruct trans-Pacific transport of dust from Asia. At the same time, they also are likely to reflect contributions of locally sourced dust. It would be valuable for future work to assess the seasonality of dust deposition from different sources, as prior work shows that Asian dust emissions peak in spring,[35] while emissions from southcentral Alaska river valleys peak in the fall.[45]

Denali snow data can be compared to paired Sr-Nd-Pb measurements on surface snow samples collected from Barrow, AK in April–May 2015, and from the Chukchi Sea sector of the Arctic Ocean (Figure 1) in August 2016 (ref.[22]), allowing for an assessment of both dust and pollution sources along a latitudinal gradient in northwestern North America. The Barrow and Arctic Ocean sites have Sr-Nd compositions similar to those from high-elevation sites in the Alaska Range, but with a greater contribution of Chinese desert dust (i.e., lower εNd, higher Sr ratios) (Figure 3). This finding is consistent with a trans-Arctic transport pathway of dust from Asia to Greenland, where the deserts of China have been inferred to be the primary source of dust.[25,26,32]

Deposition of Pollution Pb in Denali National Park and Northwestern North America. Denali snow pit Pb isotopes show a strong relationship to elevation, with more-radiogenic Pb (higher $^{206}Pb/^{204}Pb$, $^{207}Pb/^{204}Pb$, $^{208}Pb/^{204}Pb$, $^{208}Pb/^{207}Pb$, and $^{206}Pb/^{207}Pb$) values found at lower elevations (Figure 2). Base Camp (2180 m) sample compositions are consistent with primary contributions of Pb from local glaciogenic sources (Figure 4 and Figure S4). High-elevation sites are characterized by less-radiogenic Pb values of $^{206}Pb/^{204}Pb$ = 18.19–18.47, $^{207}Pb/^{204}Pb$ = 15.60–15.61, $^{208}Pb/^{204}Pb$ = 38.16–38.34, $^{206}Pb/^{207}Pb$ = 1.166–1.198, and $^{208}Pb/^{207}Pb$ = 2.446–2.464 (Figure 4 and Figure S4; Camp 14 values are revised slightly to remove contribution of Pavlof ash; see the SI). The high-elevation Pb isotopic compositions are less radiogenic than would be expected from any dust sources in Alaska or Asia and instead point to a pollution source. These samples have highly correlated $^{208}Pb/^{207}Pb$ and $^{206}Pb/^{207}Pb$ values (R^2 = 0.96), suggesting that the same primary sources are supplying Pb across a range of elevations, though in different mixing ratios.

Arctic snow samples show comparably low (less-radiogenic) Pb isotope ratios, suggesting a pollution source similar to the Denali snow samples.[22] Taken together, the data from the three sites form a tight linear array that indicates primarily two-component mixing (Figure 4B). One end-member appears to be mineral dust, with relatively high $^{206}Pb/^{207}Pb$ and $^{208}Pb/^{207}Pb$ (refs 32 and 51), while the other end-member strongly indicates a pollution source. The array of snow pit Pb isotope data extends beyond the majority of Chinese coal sources, which generally have higher $^{208}Pb/^{207}Pb$ values[52,53] compared to the Denali-Arctic Pb isotope trend (Figure 4A). Likewise, the snow pit array trends in the opposite direction from the field for North American coal sources (which plot off the chart area), which are characterized by very high $^{206}Pb/^{207}Pb$ and $^{208}Pb/^{207}Pb$ values (e.g., ~1.3 and ~2.5, respectively[54,55]). Instead, the pollution end-member supplying Pb to Denali and Arctic snow appears to be pollutant aerosols from China[43,53] with $^{206}Pb/^{207}Pb$ of 1.162 ± 0.011 (mean ± 1σ) and $^{208}Pb/^{207}Pb$ of 2.451 ± 0.014 (blue field representing 2002–2012 aerosol data in Figure 4). We explore the composition of this end-member in more detail in the section entitled 'Pb Pollution Source Apportionment'.

https://doi.org/10.1021/acs.est.2c03767
Environ. Sci. Technol. 2022, 56, 13107–13118

The Pb isotope compositions of Pb sources and aerosols from Japan, South Korea, and Russia also plot near those from China (Figure S5). Because the contributions from these other industrialized nations cannot be quantified using Pb isotope ratios, we have developed Pb emissions estimates using data for gasoline consumption, coal-burning, and non-ferrous (Cu, Ni, Pb, Zn) metal smelting, the three largest sources of Pb emissions,[56] following the approach of ref 39 (see Methods). The emissions data illustrate the predominance of Chinese Pb inputs to the North Pacific region from 1990 to 2015 (Figure 5). A lack of data from the former Soviet Union prevents a full assessment of relative contributions prior to 1990, but it is clear from Figure 5 that Chinese emissions from coal-burning and gasoline combustion both increased during the 1980s and remained well above those from Japan and South Korea.

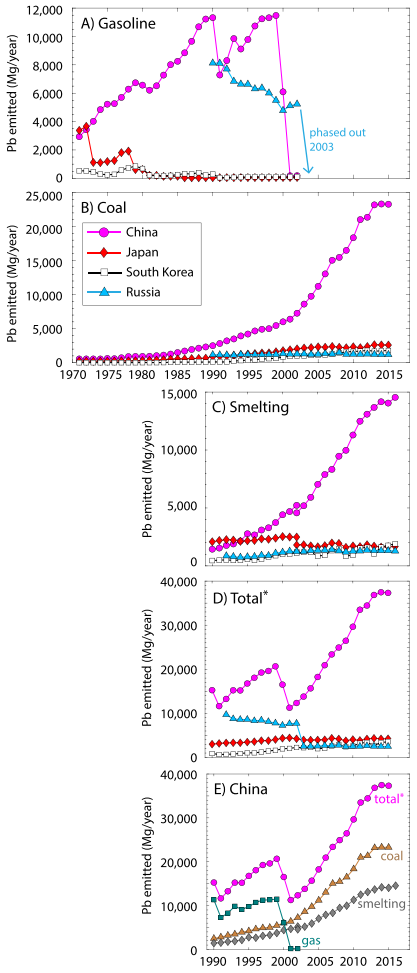

Figure 5. Atmospheric Pb emissions estimates for countries in Asia. (A) Gasoline, (B) coal-burning, and (C) smelting of Cu, Ni, Pb, and Zn ores, which comprise the three largest sources of Pb emissions over the period shown. (D) Total Pb emissions are calculated as the sum of leaded gasoline, coal-burning, and non-ferrous metal smelting emissions. *Excludes additional minor sources of Pb emissions, including iron and steel smelting, unleaded vehicle exhaust, cement production, and waste incineration.[56] (E) Comparison of Chinese Pb emissions by source. Gasoline data, coal data up to 1989, and smelting data up to 2002 are from ref 39. Offsets in panel (C) likely reflect differences in how the underlying ore data were reported, as the same approach was used to calculate Pb emissions between the two studies; see Materials and Methods and the SI for details and data sources.

Regarding Russian emissions, as of 2016, only about 1% of the total capacity (in metric tons per year) of Cu, Ni, Pb, and Zn processing plants in Russia was represented by plants in the Far East (e.g., in the Primorskiy Kray region that includes Vladivostok).[57] Likewise, the majority of Russian coal-fired power plants are located well to the west of East Asia.[58] Therefore, if anything, Figure 5D likely overestimates the potential Russian contribution to northwestern North America. What is clear from the emissions data is that China has accounted for an increasing share of total Pb emissions from this region through time, from 50 to 60% during the 1990s to 70 to 80% during 2005−2015 (Figure 5D). Based on the most recent emissions data, we estimate that China contributed ∼78% of the pollution Pb to our sample sites and to the North Pacific region more generally. The remaining portion came primarily from coal-burning and non-ferrous metal smelting in Japan and South Korea and, to a lesser extent, Russia. The interpretations based on geochemical data and emissions estimates are supported by atmospheric back-trajectory modeling (Figure S6).

Quantifying Lead Deposition in Denali National Park. To constrain the flux and the enrichment levels from pollution of Pb deposited in Denali National Park, we use data from the Denali ice core (208 m long) collected in 2013 on Mt. Hunter (3870 m, refs 20 and 21) (see the SI). We find that Pb concentrations deposited between 1991 and 2011 are very high compared to upper continental crust,[59] enriched by a factor of 3−5 relative to preindustrial times (see the SI). In other words, the ice core data suggest that about 66−80% of the Pb deposited at high elevations in Denali National Park during 1991−2011 came from anthropogenic sources. This compares to a pollution contribution estimate of >90% in the Mt. Logan ice core (5300 m) over the period 1981−1998 (ref 23), likely reflecting a smaller Pb contribution from local dust sources at the higher-elevation site. Average Pb flux for 1991−2011 on Mt. Hunter was 64−93 μg Pb m^{-2} yr^{-1}, including both crustal and anthropogenic Pb sources and excluding explosive volcanic eruptions. This compares to a preindustrial flux of 5−7 μg Pb m^{-2} $yr^{-}1$. The 1991−2011 values are likely lower than more recent Pb flux values, considering how Pb emissions have increased since 2011 (Figure 5). Given the increase in Pb emissions from China, we assume that the higher ice-core-based estimate of 80% pollution-sourced Pb on Mt. Hunter is most congruent with our 2016 results.

The ice core-based estimates of Pb flux can be used to determine the amount of pollutant Pb deposited in Denali National Park over the period 1991−2011 (see the SI). Applying the Mt. Hunter pollution estimate of 80% yields an annual pollutant Pb flux of 51−74 μg m^{-2} yr^{-1}. This range is comparable to other flux estimates in the northeast Pacific. For instance, Pb flux over the period 1981−1998 on Mt. Logan was 26 μg m^{-2} yr^{-1} while the Eclipse ice core recorded about 900 μg m^{-2} yr^{-1} across the same interval,[11,23] likely reflecting a larger flux of local terrestrial dust. The Denali total Pb flux of 64−93 μg Pb m^{-2} yr^{-1} is comparable to that recorded at the PARCA Act2 site in south-central Greenland during peak 20th century pollution (1950−1975 average), where a total Pb flux including natural and anthropogenic sources of 91 μg m^{-2} yr^{-1} was recorded.[8,9,23] Thus, Pb aerosol deposition in northwestern North America roughly equals that in southern Greenland during peak pollution from North American leaded gasoline emissions, despite a longer transport distance across the Pacific

https://doi.org/10.1021/acs.est.2c03767
Environ. Sci. Technol. 2022, 56, 13107−13118

and the phasing out of leaded gasoline in both China and Russia.

Pb Pollution Source Apportionment. Using the Pb enrichment values, we can independently calculate the expected Pb isotopic composition of the pollution end-member (Figure 4B). This is possible because the Sr-Nd isotope data provide the approximate proportions of local Alaska and long-range transported dust (e.g., 60% Alaska, 40% China; Table S2), and the linear nature of the snow pit Pb isotope data array further constrains the Pb isotope composition of the dust end-member. Using the median values for China and Alaska dust sources, we calculate a mixed-dust end-member with $^{208}Pb/^{207}Pb = 2.476$ and $^{206}Pb/^{207}Pb = 1.213$ (Figure 4B). We can then use this dust end-member, along with the proportion of pollution Pb estimated for Mt. Hunter, to calculate the pollution end-member composition. By mass balance (shown for $^{206}Pb/^{207}Pb$), $^{206}Pb/^{207}Pb_{Sample} = {}^{206}Pb/^{207}Pb_{Pollution} \times f + {}^{206}Pb/^{207}Pb_{Dust}(1 - f)$, where f is the fraction of Pb from pollution (0.8 on Mt. Hunter). Since the Pb isotope ratio of the pollutant is the unknown in this case, we can rearrange the equation to calculate it: $^{206}Pb/^{207}Pb_{Pollution} = [{}^{206}Pb/^{207}Pb_{Sample} - {}^{206}Pb/^{207}Pb_{Dust}(1 - f)]/f$. We find that the Pb isotope ratios of the pollution source to Denali are $^{208}Pb/^{207}Pb = 2.439$ and $^{206}Pb/^{207}Pb = 1.154$. Because the Pb isotope compositions of the two dust sources are very similar, the specific values used for each dust source (median vs extreme high or extreme low Pb isotope ratios) make little difference in the calculated pollution end-member. The composition of our calculated pollution end-member plots within the field for modern (2002−2012) urban aerosols in China[43,53] (Figure 4A), strengthening our interpretation that Chinese air pollution is the primary pollution source of Pb to our samples.

Recognizing that air pollution inherently represents a mixture of sources, we wanted to quantify the contributions of Pb from coal-burning and non-ferrous metal smelting to the calculated pollution end-member as these two sources represent the main contributors of Pb emissions following the phase-out of leaded gasoline in China. We used MixSIAR, an advanced Bayesian isotope mixing model,[60−62] to quantify the contributions of Pb from Chinese ore and coal sources to our calculated pollution end-member (see the SI). The end-member values are defined as the mean ± 1σ of the published data for each source (Table S1, Figure 4 and Figure S5). The model indicates that a median of 19% (1σ range: 11−27%) comes from ore bodies with $^{206}Pb/^{207}Pb$ of ∼0.98−1.08 and $^{208}Pb/^{207}Pb$ of ∼2.25−2.44, which we term 'ore 1'; 49% (26−72%) of the Pb comes from ore bodies with $^{206}Pb/^{207}Pb$ of ∼1.13−1.18 and $^{208}Pb/^{207}Pb$ of ∼2.45−2.49, which we term 'ore 2'; and 31% (10−52%) comes from coal-burning. The uncertainty in the Pb isotopic composition of the pollution end-member is much smaller than the uncertainty in the model results, likely reflecting the large range of compositions within Chinese ore and coal fields (Figure 4A). Pollution aerosols in China thus represent multiple sources of Pb with a large range of compositions.

Considering that our samples plot in a linear array between the mixed-dust end-member and the pollution end-member, we can calculate the proportion of Pb sourced from pollution to each sample by solving for the pollution fraction f and then apply the modeled proportions of Chinese ore and coal-derived Pb based on the modeling results. We assume that Pb emissions from Japan, Korea, and Russia together account for 22% of the pollution contribution to each sample, based on the Pb emissions estimates for 2015 (Figure 5D). The remainder of the pollution contribution, representing 21−64% of the Pb delivered to high-elevation sites in Denali National Park, depending on the site, comes from Chinese pollution sources (Figure 6). Results for the Barrow and Arctic Ocean sites[22] are

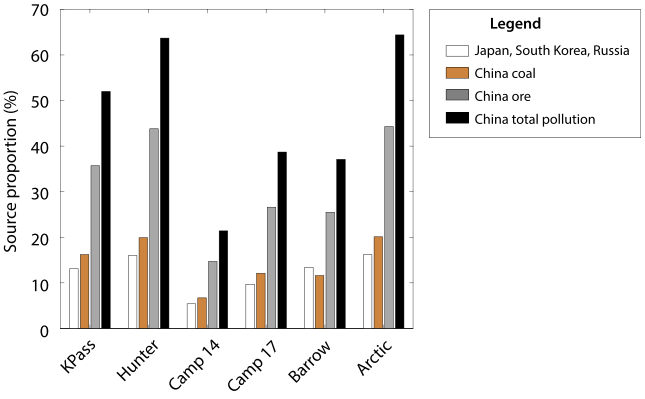

Figure 6. Bar plot showing median source proportions of pollution Pb calculated for each site. The major portion (21−64%) of pollution Pb deposited in high-elevation and high-latitude sites can be attributed to Chinese pollution sources, with lesser contributions (totaling 5−16%) from Japan, South Korea, and Russia. The Barrow and Arctic Ocean data are from ref 22.

comparable to the Denali snow pits, with 37% and 64% of their Pb sourced from China, respectively. Our results, showing that the major proportion of Pb deposited at high elevations and high latitudes in northwestern North America comes from Chinese pollution sources (Figure 6), are likely representative of high-altitude aerosol transport in the North Pacific and western Arctic more generally and provide an important geochemical benchmark for future studies.

Increasing Influence of Chinese Pollution in Northwestern North America and the Western Arctic. Over the past four decades, Pb aerosols in northwestern North America and across the western Arctic have increasingly been influenced by the trans-Pacific transport of East Asian pollution. This is evident from both Pb emissions estimates (Figure 5) and from environmental archives. The timing and pace of industrialization in East Asian nations have differed, and these different histories are recorded by natural archives, including ice cores,[11,23,27] corals,[63] and North Pacific ocean waters.[39,64] Ice core records from the St. Elias mountains (Figure 1), including from the Mt. Logan ice core (5300 m asl, spanning through 1998 C.E.) and Eclipse ice core (3017 m asl, 1970−2001 C.E.), show Pb concentrations increasing in parallel with Chinese industrialization during the late 20th century. The Mt. Logan ice core shows that anthropogenic Pb deposition increased markedly after 1950 with post-World War II industrialization, while the largest jump to values ten times above the pre-industrial baseline occurred in the 1980s.[23] Over the period 1970−2001, Eclipse ice core Pb isotope analyses indicate contributions from both East Asia (China and Japan) and from North America, with an increasing Asian pollution signal through time[11] (the Mt. Logan record does not include Pb isotopes). Lead isotope data from the Ogasawara coral record from Japan show that Japanese Pb emissions dominated deposition in that part of the northwest Pacific through much

https://doi.org/10.1021/acs.est.2c03767
Environ. Sci. Technol. 2022, 56, 13107−13118

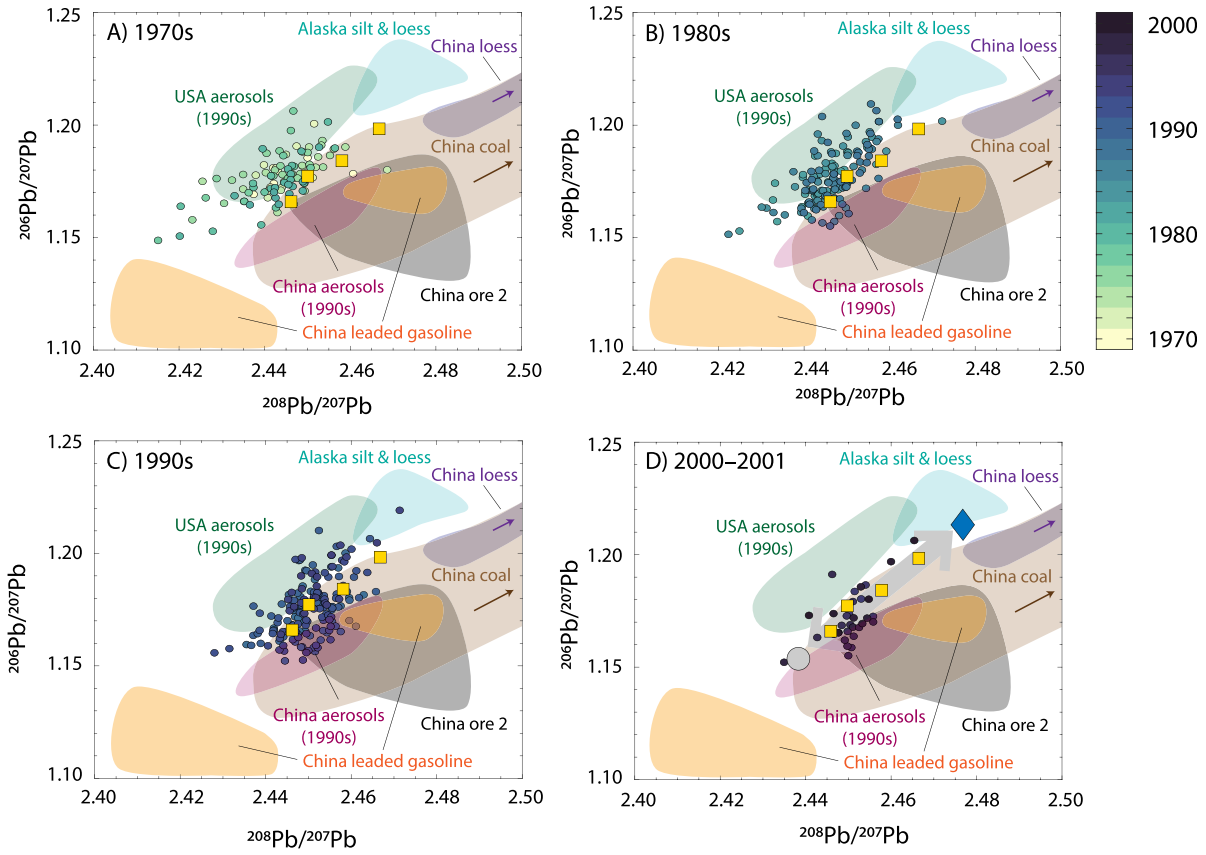

Figure 7. Comparison of Denali high-elevation snow pit Pb isotope compositions from 2016 (yellow squares) with Eclipse Icefield ice core data[11] (circles, color bar in years C.E.). Panels show the progressive shift toward higher $^{208}Pb/^{207}Pb$ values over the past 50 years including (A) 1970s, (B), 1980s, (C), 1990s, and (D) 2000–2001. Panel (D) shows the mixed-dust end-member (teal diamond) and pollution end-member (gray circle) inferred for the Denali samples. Error bars for the Denali samples are smaller than the symbol size. Eclipse error bars can be seen in Figure S7. Source data citations are the same as in Figure 4.

of the 20th century.[63] However, beginning in 1980, Pb concentrations and $^{208}Pb/^{207}Pb$ ratios increased, signaling the rapid industrialization of China.[63] By the end of the Ogasawara record in 2001, 64 ± 14% of Pb deposition at that location could be attributed to Chinese sources.[63] Lead isotope data from the northwest Pacific Ocean surface mixed layer (max depth ranging from 12–110 m, interpreted to represent a 5-year integrated signal, i.e., ~1997–2002) are indistinguishable from Chinese aerosol data.[39] By coupling Pb isotope data with emissions estimates, the authors determined that Chinese emissions accounted for the majority of Pb deposition in the northwest Pacific, with lesser contributions from Russia and Japan (other countries' inputs were considered minimal).[39] Overall, Pb data from across the North Pacific region show that China has been the dominant source of Pb pollution since the 1990s. On a broader scale, aerosol measurements made across the continental U.S. show that Pb pollution sources to the western and eastern US began to differ in the 1990s, a shift attributed to an increasing proportion of Chinese industrial Pb pollution following the elimination of leaded gasoline in the US.[47] As of 2008, Chinese aerosols contributed a median of ~30% of Pb pollution to sites in northern California.[43]

Comparison of the high-elevation Denali snow pit data with the Pb isotope record from the Eclipse ice core[11] demonstrates the changing history of Pb pollution in northwestern North America (Figure 7, Eclipse error bars are shown in Figure S7). During the 1970s, the Eclipse record was largely influenced by pollution aerosols from the US (Figure 7A). Beginning in the 1980s, the increasing influence of Chinese industrialization can be seen as a shift toward higher $^{208}Pb/^{207}Pb$ values (Figure 7B), with Eclipse data overlapping the field of Chinese urban aerosols.[47] During the 1990s, the Eclipse data span the fields of U.S. and Chinese aerosols and bracket the range of Denali snow values from this study (Figure 7C). By the end of the Eclipse ice core record in 2001, the Eclipse data plot almost entirely within the Chinese source fields, with most data indistinguishable from Chinese urban aerosols (Figure 7D). The Eclipse data overlap the data from two of the highest-elevation Denali snow pits, which according to Denali ice core Pb enrichment data receive up to 80% of their Pb from pollution sources. Together these records, along with the data from Barrow and the Arctic Ocean,[22] demonstrate the pervasive trans-Pacific deposition of Chinese pollution aerosols in northwestern North America.

On the opposite side of North America, ice cores from Greenland document changing European Pb emissions over the past nearly three millennia, including significant Pb emissions from North America, which peaked during the mid-20th century.[8,65,66] However, recent Greenland snow samples register the imprint of Chinese pollution. Beginning in the late 1990s, about 50% of Pb deposition in central Greenland[27] and up to 73% of Pb deposition in northwestern Greenland[28] could be attributed to Chinese pollution sources. Thus, across the western Arctic from Alaska to Greenland, Pb isotopes reflect the substantial and increasing influence of pollutant aerosols from China. In contrast, ice core records

https://doi.org/10.1021/acs.est.2c03767
Environ. Sci. Technol. 2022, 56, 13107–13118

from the European Alps[10] and Altai[67] document declining Pb emissions from Western and Eastern Europe related to the phasing out of leaded gasoline and economic collapse of the Soviet Union, respectively. These records, along with those from Greenland[8,9] and Devon Island,[24] highlight the positive and ongoing impact of Pb abatement measures.

The new data from Denali are among the first from northwestern North America that demonstrate potential changes in the Pb isotope compositions of long-range-transported aerosols following the 2001 phase-out of leaded gasoline in China. A comparison of our 2016 samples with the most recent samples from the Eclipse ice core (e.g., 2000−2001; Figure 7D) demonstrates similarities in their Pb isotope compositions, indicating that the isotopic signature of long-range-transported pollutants remained fairly stable over the past two decades in spite of the phase-out of leaded gasoline in China. This likely reflects the fact that Chinese tetraethyl Pb made use of locally sourced Pb ore, which continues to be emitted through smelting and other industrial activities. This can be seen in the overlapping fields for leaded gasoline and 'ore 2' (Figure 7) as well as the second field for leaded gasoline, which plots near 'ore 1' (the latter field is just off the lower axis bounds in Figure 7). Consistent with this interpretation, North Pacific shallow ocean Pb concentrations from the early 2000s suggest that industrial emissions had more than compensated for the decline in leaded gasoline emissions.[39] This conclusion is corroborated by Pb emissions data, which show that by 2006, total Chinese emissions had rebounded from the dip due to the phase-out of tetraethyl Pb. From 2006 to 2014, emissions increased sharply, reaching over 37,000 metric tons of Pb per year (Figure 5). The 2015 data show a slight decrease, likely reflecting significant Chinese governmental efforts to abate Pb emissions.[68] It can be hoped that as new emissions data become available, a downward trend will emerge.

While aerosols measured in China show a slight shift toward higher $^{206}Pb/^{207}Pb$ and lower $^{208}Pb/^{206}Pb$ values (i.e., from a more "ore-like" to a more "coal-like" composition) following the gasoline Pb additive ban,[53] our data indicate that the ban did not have a significant impact on long-range pollutant Pb isotope compositions. This finding, though surprising, parallels results from the Devon Ice Cap in the eastern Canadian Arctic, where ice core Pb isotope data showed no change following the leaded gasoline bans in North America (1970) and Europe (1980)[24] despite declining Pb deposition. Together, these studies show that remote locations across the Arctic continue to accumulate anthropogenic heavy metal pollutants from distal locations. Although Pb deposition rates in the Arctic from Asian pollution sources are not high enough to be considered toxic,[69] data from remote locations serve as an important testament to the global nature of heavy metal pollution. While the complete global phase-out of leaded gasoline[5] represents a victory for human health and the environment, our results suggest that some of the benefits of banning Pb additives from gasoline have been short-lived as other industrial uses of Pb have increased over the past two decades. Further efforts are needed to decrease Pb emissions to reduce impacts of Pb on vulnerable children, particularly in developing nations.[70]

■ ASSOCIATED CONTENT

Supporting Information

The Supporting Information is available free of charge at https://pubs.acs.org/doi/10.1021/acs.est.2c03767.

Additional information on sample collection and processing, assessment of grain size and potential input of ash from the March 2016 Pavlof eruption, method for estimating the non-volcanic composition of the Camp 14 sample, analytical methods for major/trace element and radiogenic isotope analysis, description of ice core Pb flux and enrichment calculations, approach for estimating Pb emissions, detailed geochemical characterization of southcentral Alaska dust source region, and seven additional figures and two tables (PDF)

■ AUTHOR INFORMATION

Corresponding Authors

Bess G. Koffman − *Department of Geology, Colby College, Waterville, Maine 04901, United States;* orcid.org/0000-0002-9451-4138; Email: bkoffman@colby.edu

Yue Cai − *State Key Laboratory of Paleobiology and Stratigraphy, Nanjing Institute of Geology and Paleontology, Chinese Academy of Sciences, Nanjing, Jiangsu Province 210008, P.R. China; Lamont-Doherty Earth Observatory of Columbia University, Palisades, New York 10964, United States;* orcid.org/0000-0002-2318-2359; Email: cai@nigpas.ac.cn

Authors

Patrick Saylor − *National Center for Atmospheric Research, Boulder, Colorado 80307, United States; Earth Science Department, Dartmouth College, Hanover, New Hampshire 03755, United States*

Roujia Zhong − *Department of Computer Science, Colby College, Waterville, Maine 04901, United States*

Lily Sethares − *Department of Geology, Colby College, Waterville, Maine 04901, United States*

Meg F. Yoder − *Department of Geology, Colby College, Waterville, Maine 04901, United States; Department of Earth and Environmental Sciences, Boston College, Boston, Massachusetts 02467, United States*

Lena Hanschka − *Department of Geology, Colby College, Waterville, Maine 04901, United States*

Taylor Methven − *Department of Geology, Colby College, Waterville, Maine 04901, United States*

Louise Bolge − *Lamont-Doherty Earth Observatory of Columbia University, Palisades, New York 10964, United States*

Jack Longman − *Institute for Chemistry and Biology of the Marine Environment, University of Oldenburg, 26129 Oldenburg, Germany*

Steven L. Goldstein − *Lamont-Doherty Earth Observatory of Columbia University, Palisades, New York 10964, United States; Department of Earth and Environmental Sciences, Columbia University, New York, New York 10027, United States*

Erich C. Osterberg − *Earth Science Department, Dartmouth College, Hanover, New Hampshire 03755, United States*

Complete contact information is available at: https://pubs.acs.org/10.1021/acs.est.2c03767

Notes

The authors declare no competing financial interest.

■ ACKNOWLEDGMENTS

The authors gratefully acknowledge support from Colby College, the Buck Lab for Climate and Environment, the Dartmouth College Society of Fellows, the Storke Endowment of the Columbia Department of Earth and Environmental Sciences, and the American Association of University Women (AAUW), which made this work possible. We thank Colby undergraduate Red Fong and Dartmouth undergraduates Rachel Rubin and Shoshanna Geller for their assistance in the lab. Thanks to Karina Graeter, Erin McConnell, Zayta Thundercloud, Dominic Winski, and David Polashenski for help with field sampling, and to Michael Handley for help with analyses. We appreciate Karl Kreutz and Hanna Brooks for helpful conversations. Thanks go to Peter Neff for assistance with HYSPLIT. We thank three anonymous reviewers for their thoughtful reviews of the manuscript, which clarified and strengthened the final paper. The authors declare no competing financial interests.

■ REFERENCES

(1) Canfield, R. L.; Henderson, C. R., Jr.; Cory-Slechta, D. A.; Cox, C.; Jusko, T. A.; Lanphear, B. P. Intellectual impairment in children with blood lead concentrations below 10 μg per deciliter. *N. Engl. J. Med.* **2003**, *348*, 1517−1526.

(2) Pourrut, B.; Shahid, M.; Dumat, C.; Winterton, P.; Pinelli, E. Lead Uptake, Toxicity, and Detoxification in Plants. In *Reviews of Environmental Contamination and Toxicology Volume 213*; Whitacre, D. M., Ed. Springer New York: New York, NY, 2011; pp. 113−136.

(3) Patterson, C. C. Contaminated and Natural Lead Environments of Man. *Arch. Environ. Health* **1965**, *11*, 344−360.

(4) Nriagu, J. O. A history of global metal pollution. *Science* **1996**, *272*, 223−223.

(5) Lobet, I. *Finally, the end of leaded gas*. https://www.nationalgeographic.com/environment/article/finally-the-end-of-leaded-gas?loggedin=true (accessed 2 February 2022).

(6) Pacyna, J. M.; Pacyna, E. G.; Aas, W. Changes of emissions and atmospheric deposition of mercury, lead, and cadmium. *Atmos. Environ.* **2009**, *43*, 117−127.

(7) Cheng, H.; Hu, Y. Lead (Pb) isotopic fingerprinting and its applications in lead pollution studies in China: a review. *Environ. Pollut.* **2010**, *158*, 1134−1146.

(8) McConnell, J. R.; Edwards, R. Coal burning leaves toxic heavy metal legacy in the Arctic. *Proc. Natl. Acad. Sci. U. S. A.* **2008**, *105*, 12140−12144.

(9) McConnell, J.; Kipfstuhl, S.; Fischer, H. The NGT and PARCA shallow ice core arrays in Greenland: A brief overview. *PAGES news* **2006**, *14*, 13−14.

(10) Schwikowski, M.; Barbante, C.; Doering, T.; Gaeggeler, H. W.; Boutron, C.; Schotterer, U.; Tobler, L.; Van de Velde, K.; Ferrari, C.; Cozzi, G. Post-17th-century changes of European lead emissions recorded in high-altitude alpine snow and ice. *Environ. Sci. Technol.* **2004**, *38*, 957−964.

(11) Gross, B. H.; Kreutz, K. J.; Osterberg, E. C.; McConnell, J. R.; Handley, M.; Wake, C.; Yalcin, K. Constraining recent lead pollution sources in the North Pacific using ice core stable lead isotopes. *J. Geophys. Res.: Atmos.* **2012**, *117* (), DOI: 10.1029/2011JD017270.

(12) Zdanowicz, C. M.; Hall, G.; Vaive, J.; Amelin, Y.; Percival, J.; Girard, I.; Biscaye, P. E.; Bory, A. J.-M. Asian dustfall in the St. Elias Mountains, Yukon, Canada. *Geochim. Cosmochim. Acta* **2006**, *70*, 3493−3507.

(13) Mahowald, N.; Albani, S.; Kok, J. F.; Engelstaedter, S.; Scanza, R.; Ward, D. S.; Flanner, M. G. The size distribution of desert dust aerosols and its impact on the Earth system. *Aeolian Res.* **2014**, 53−71.

(14) Adebiyi, A. A.; Kok, J. F. Climate models miss most of the coarse dust in the atmosphere. *Sci. Adv.* **2020**, *6*, No. eaaz9507.

(15) Boyd, P. W.; Jickells, T.; Law, C.; Blain, S.; Boyle, E.; Buesseler, K.; Coale, K.; Cullen, J.; De Baar, H. J.; Follows, M. Mesoscale iron enrichment experiments 1993-2005: synthesis and future directions. *Science* **2007**, *315*, 612−617.

(16) Martin, J. H.; Fitzwater, S. E. Iron deficiency limits phytoplankton growth in the north-east Pacific subarctic. *Nature* **1988**, *331*, 341−343.

(17) Roberts, G.; Mauger, G.; Hadley, O.; Ramanathan, V. North American and Asian aerosols over the eastern Pacific Ocean and their role in regulating cloud condensation nuclei. *J. Geophys. Res.: Atmos.* **2006**, *111* (), DOI: 10.1029/2005JD006661.

(18) Twohy, C. H.; Kreidenweis, S. M.; Eidhammer, T.; Browell, E. V.; Heymsfield, A. J.; Bansemer, A. R.; Anderson, B. E.; Chen, G.; Ismail, S.; DeMott, P. J. Saharan dust particles nucleate droplets in eastern Atlantic clouds. *Geophys. Res. Lett.* **2009**, *36* (), DOI: 10.1029/2008GL035846.

(19) Creamean, J. M.; Suski, K. J.; Rosenfeld, D.; Cazorla, A.; DeMott, P. J.; Sullivan, R. C.; White, A. B.; Ralph, F. M.; Minnis, P.; Comstock, J. M. Dust and biological aerosols from the Sahara and Asia influence precipitation in the western US. *Science* **2013**, *339*, 1572−1578.

(20) Osterberg, E. C.; Winski, D. A.; Kreutz, K. J.; Wake, C. P.; Ferris, D. G.; Campbell, S.; Introne, D.; Handley, M.; Birkel, S. D. The 1200 year composite ice core record of Aleutian Low intensification. *Geophys. Res. Lett.* **2017**, *44*, 7447.

(21) Winski, D.; Osterberg, E.; Ferris, D.; Kreutz, K.; Wake, C.; Campbell, S.; Hawley, R.; Roy, S.; Birkel, S. D.; Introne, D.; Handley, M. Industrial-age doubling of snow accumulation in the Alaska Range linked to tropical ocean warming. *Sci. Rep.* **2017**, *7*, 17869.

(22) Du, Z.; Xiao, C.; Dou, T.; Li, S.; An, H.; Liu, S.; Liu, K. Comparison of Sr−Nd−Pb isotopes in insoluble dust between northwestern China and high-latitude regions in the Northern Hemisphere. *Atmos. Environ.* **2019**, *214*, 116837.

(23) Osterberg, E. C.; Mayewski, P.; Kreutz, K.; Fisher, D.; Handley, M.; Sneed, S. B.; Zdanowicz, C. M.; Zheng, J.; Demuth, M.; Waskiewicz, M.; Bourgeois, J. Ice core record of rising lead pollution in the North Pacific atmosphere. *Geophys. Res. Lett.* **2008**, *35* (), DOI: 10.1029/2007GL032680.

(24) Shotyk, W.; Zheng, J.; Krachler, M.; Zdanowicz, C.; Koerner, R.; Fisher, D. Predominance of industrial Pb in recent snow (1994−2004) and ice (1842−1996) from Devon Island, Arctic Canada. *Geophys. Res. Lett.* **2005**, *32* (), DOI: 10.1029/2005GL023860.

(25) Bory, A. J.-M.; Biscaye, P. E.; Svensson, A.; Grousset, F. Seasonal variability in the origin of recent atmospheric mineral dust at NorthGrIP, Greenland. *Earth Planet. Sci. Lett.* **2002**, *196*, 123−134.

(26) Bory, A.; Biscaye, P. E.; Piotrowski, A.; Steffensen, J. P., Regional variability of ice core dust composition and provenance in Greenland. *Geochemistry*; Geophysics, Geosystems 2003.

(27) Bory, A. J.-M.; Abouchami, W.; Galer, S. J.; Svensson, A.; Christensen, J. N.; Biscaye, P. E. A Chinese imprint in insoluble pollutants recently deposited in central Greenland as indicated by lead isotopes. *Environ. Sci. Technol.* **2014**, *48*, 1451−1457.

(28) Kang, J.-H.; Hwang, H.; Han, C.; Do Hur, S.; Kim, S.-J.; Hong, S. Pb concentrations and isotopic record preserved in northwest Greenland snow. *Chemosphere* **2017**, *187*, 294−301.

(29) Grousset, F. E.; Biscaye, P. E. Tracing dust sources and transport patterns using Sr, Nd and Pb isotopes. *Chem. Geol.* **2005**, *222*, 149−167.

(30) Garçon, M.; Chauvel, C.; France-Lanord, C.; Limonta, M.; Garzanti, E. Which minerals control the Nd-Hf-Sr-Pb isotopic compositions of river sediments? *Chem. Geol.* **2014**, *364*, 42−55.

(31) Feng, J.-L.; Hu, Z.-G.; Cui, J.-Y.; Zhu, L.-P. Distributions of lead isotopes with grain size in aeolian deposits. *Terra Nova* **2010**, *22*, 257−263.

(32) Biscaye, P. E.; Grousset, F. E.; Revel, M.; Van der Gaast, S.; Zielinski, G. A.; Vaars, A.; Kukla, G. Asian provenance of glacial dust

(stage 2) in the Greenland Ice Sheet Project 2 ice core, Summit, Greenland. *J. Geophys. Res.* **1997**, *102*, 26765−26781.
(33) Koffman, B. G.; Yoder, M. F.; Methven, T.; Hanschka, L.; Sears, H. B.; Saylor, P.; Wallace, K. L. Glacial dust surpasses both volcanic ash and desert dust in its iron fertilization potential. *Global Biogeochem. Cycles* **2021**, *35*, 32020GB0006821.
(34) Koffman, B. G.; Yoder, M. F.; Methven, T.; Hanschka, L.; Sears, H. B.; Saylor, P. L.; Wallace, K. L. *Geochemistry of sediments and volcanic ash from Southcentral Alaska*, Version 1.0. Interdisciplinary Earth Data Alliance (IEDA). 2021.
(35) Fischer, E. V.; Hsu, N. C.; Jaffe, D. A.; Jeong, M.-J.; Gong, S. L. A decade of dust: Asian dust and springtime aerosol load in the U.S. Pacific Northwest. *Geophys. Res. Lett.* **2009**, *36* (), DOI: 10.1029/2008GL036467.
(36) Osterberg, E. C.; Handley, M. J.; Sneed, S. B.; Mayewski, P. A.; Kreutz, K. J. Continuous ice core melter system with discrete sampling for major ion, trace element, and stable isotope analyses. *Environ. Sci. Technol.* **2006**, *40*, 3355−3361.
(37) Breton, D. J.; Koffman, B. G.; Kurbatov, A. V.; Kreutz, K. J.; Hamilton, G. S. Quantifying signal dispersion in a hybrid ice core melting system. *Environ. Sci. Technol.* **2012**, *46*, 11922−11928.
(38) Koffman, B. G.; Handley, M. J.; Osterberg, E. C.; Wells, M. L.; Kreutz, K. J. Dependence of ice-core relative trace-element concentration on acidification. *J. Glaciol.* **2014**, *60*, 103.
(39) Zurbrick, C. M.; Gallon, C.; Flegal, A. R. Historic and industrial lead within the Northwest Pacific Ocean evidenced by lead isotopes in seawater. *Environ. Sci. Technol.* **2017**, *51*, 1203−1212.
(40) Stone, R.; Anderson, G.; Andrews, E.; Dutton, E.; Shettle, E.; Berk, A. Incursions and radiative impact of Asian dust in northern Alaska. *Geophys. Res. Lett.* **2007**, *34* (), DOI: 10.1029/2007GL029878.
(41) Uno, I.; Eguchi, K.; Yumimoto, K.; Takemura, T.; Shimizu, A.; Uematsu, M.; Liu, Z.; Wang, Z.; Hara, Y.; Sugimoto, N. Asian dust transported one full circuit around the globe. *Nat. Geosci.* **2009**, *2*, 557.
(42) Yumimoto, K.; Eguchi, K.; Uno, I.; Takemura, T.; Liu, Z.; Shimizu, A.; Sugimoto, N.; Strawbridge, K. Summertime trans-Pacific transport of Asian dust. *Geophys. Res. Lett.* **2010**, *37* (), DOI: 10.1029/2010GL043995.
(43) Ewing, S. A.; Christensen, J. N.; Brown, S. T.; Vancuren, R. A.; Cliff, S. S.; Depaolo, D. J. Pb isotopes as an indicator of the Asian contribution to particulate air pollution in urban California. *Environ. Sci. Technol.* **2010**, *44*, 8911−8916.
(44) Wu, Y.; Han, Z.; Nazmi, C.; Gross, B.; Moshary, F. A trans-Pacific Asian dust episode and its impacts to air quality in the east coast of US. *Atmos. Environ.* **2015**, *106*, 358−368.
(45) Crusius, J.; Schroth, A. W.; Gasso, S.; Moy, C. M.; Levy, R. C.; Gatica, M. Glacial flour dust storms in the Gulf of Alaska: Hydrologic and meteorological controls and their importance as a source of bioavailable iron. *Geophys. Res. Lett.* **2011**, *38* (), DOI: 10.1029/2010GL046573.
(46) Crusius, J. Dissolved Fe supply to the central Gulf of Alaska is inferred to be derived from Alaskan glacial dust that is not resolved by dust transport models. *J. Geophys. Res.: Biogeosci.* **2021**, e2021JG006323.
(47) Bollhöfer, A.; Rosman, K. Isotopic source signatures for atmospheric lead: the Northern Hemisphere. *Geochim. Cosmochim. Acta* **2001**, *65*, 1727−1740.
(48) Díaz-Somoano, M.; Kylander, M. E.; López-Antón, M. A.; Suárez-Ruiz, I.; Martínez-Tarazona, M. R.; Ferrat, M.; Kober, B.; Weiss, D. J. Stable lead isotope compositions in selected coals from around the world and implications for present day aerosol source tracing. *Environ. Sci. Technol.* **2009**, *43*, 1078−1085.
(49) Nakano, T.; Yokoo, Y.; Nishikawa, M.; Koyanagi, H. Regional Sr−Nd isotopic ratios of soil minerals in northern China as Asian dust fingerprints. *Atmos. Environ.* **2004**, *38*, 3061−3067.
(50) Chen, J.; Li, G.; Yang, J.; Rao, W.; Lu, H.; Balsam, W.; Sun, Y.; Ji, J. Nd and Sr isotopic characteristics of Chinese deserts: implications for the provenances of Asian dust. *Geochim. Cosmochim. Acta* **2007**, *71*, 3904−3914.
(51) Jones, C. E.; Halliday, A. N.; Rea, D. K.; Owen, R. M. Eolian inputs of lead to the North Pacific. *Geochim. Cosmochim. Acta* **2000**, *64*, 1405−1416.
(52) Mukai, H.; Furuta, N.; Fujii, T.; Ambe, Y.; Sakamoto, K.; Hashimoto, Y. Characterization of sources of lead in the urban air of Asia using ratios of stable lead isotopes. *Environ. Sci. Technol.* **1993**, *27*, 1347−1356.
(53) Bi, X.-Y.; Li, Z.-G.; Wang, S.-X.; Zhang, L.; Xu, R.; Liu, J.-L.; Yang, H.-M.; Guo, M.-Z. Lead isotopic compositions of selected coals, Pb/Zn ores and fuels in China and the application for source tracing. *Environ. Sci. Technol.* **2017**, *51*, 13502−13508.
(54) Chow, T. J.; Earl, J. L. Lead isotopes in North American coals. *Science* **1972**, *176*, 510−511.
(55) Sangster, D.; Outridge, P.; Davis, W. Stable lead isotope characteristics of lead ore deposits of environmental significance. *Environ. Rev.* **2000**, *8*, 115−147.
(56) Li, Q.; Cheng, H.; Zhou, T.; Lin, C.; Guo, S. The estimated atmospheric lead emissions in China, 1990−2009. *Atmos. Environ.* **2012**, *60*, 1−8.
(57) Survey, U. S. G. *Minerals Yearbook, Volume I, Metals and Minerals*; 2016.
(58) Evans, S.; Pearce, R. *Mapped: The world's coal power plants. Carbon Brief*, 2019; pp https://www.carbonbrief.org/mapped-worlds-coal-power-plants, accessed 2022-03-31.
(59) Wedepohl, K. H. The composition of the continental crust. *Geochim. Cosmochim. Acta* **1995**, *59*, 1217−1232.
(60) Stock, B. C.; Jackson, A. L.; Ward, E. J.; Parnell, A. C.; Phillips, D. L.; Semmens, B. X. Analyzing mixing systems using a new generation of Bayesian tracer mixing models. *PeerJ* **2018**, *6*, No. e5096.
(61) Longman, J.; Veres, D.; Ersek, V.; Phillips, D. L.; Chauvel, C.; Tamas, C. G. Quantitative assessment of Pb sources in isotopic mixtures using a Bayesian mixing model. *Sci. Rep.* **2018**, *8*, 1−16.
(62) Longman, J.; Struve, T.; Pahnke, K. Spatial and temporal trends in mineral dust provenance in the South Pacific−evidence from mixing models. *Paleoceanography Paleoclimatology* **2022**, No. e2021PA004356.
(63) Inoue, M.; Tanimizu, M. Anthropogenic lead inputs to the western Pacific during the 20th century. *Sci. Total Environ.* **2008**, *406*, 123−130.
(64) Gallon, C.; Ranville, M. A.; Conaway, C. H.; Landing, W. M.; Buck, C. S.; Morton, P. L.; Flegal, A. R. Asian industrial lead inputs to the North Pacific evidenced by lead concentrations and isotopic compositions in surface waters and aerosols. *Environ. Sci. Technol.* **2011**, *45*, 9874−9882.
(65) McConnell, J. R.; Wilson, A. I.; Stohl, A.; Arienzo, M. M.; Chellman, N. J.; Eckhardt, S.; Thompson, E. M.; Pollard, A. M.; Steffensen, J. P. Lead pollution recorded in Greenland ice indicates European emissions tracked plagues, wars, and imperial expansion during antiquity. *Proc. Natl. Acad. Sci. U. S. A.* **2018**, *115*, 5726−5731.
(66) McConnell, J. R.; Chellman, N. J.; Wilson, A. I.; Stohl, A.; Arienzo, M. M.; Eckhardt, S.; Fritzsche, D.; Kipfstuhl, S.; Opel, T.; Place, P. F.; Steffensen, J. P. Pervasive Arctic lead pollution suggests substantial growth in medieval silver production modulated by plague, climate, and conflict. *Proc. Natl. Acad. Sci. U. S. A.* **2019**, *116*, 14910−14915.
(67) Eichler, A.; Tobler, L.; Eyrikh, S.; Gramlich, G.; Malygina, N.; Papina, T.; Schwikowski, M. Three centuries of Eastern European and Altai lead emissions recorded in a Belukha ice core. *Environ. Sci. Technol.* **2012**, *46*, 4323−4330.
(68) He, K.; Huo, H.; Zhang, Q. Urban air pollution in China: current status, characteristics, and progress. *Annu. Rev. Energy* **2002**, *27*, 397−431.
(69) Van Oostdam, J.; Donaldson, S. G.; Feeley, M.; Arnold, D.; Ayotte, P.; Bondy, G.; Chan, L.; Dewaily, E.; Furgal, C.; Kuhnlein, H. Human health implications of environmental contaminants in Arctic Canada: a review. *Sci. Total Environ.* **2005**, *351*, 165−246.

(70) Han, Z.; Guo, X.; Zhang, B.; Liao, J.; Nie, L. Blood lead levels of children in urban and suburban areas in China (1997−2015): Temporal and spatial variations and influencing factors. *Sci. Total Environ.* **2018**, *625*, 1659−1666.

https://doi.org/10.1021/acs.est.2c03767
Environ. Sci. Technol. 2022, 56, 13107−13118